Early endosomes associated with dynamic F-actin structures are required for late trafficking of *H. pylori* VacA toxin

Nils C. Gauthier,[1] Pascale Monzo,[2] Teresa Gonzalez,[2] Anne Doye,[1] Amanda Oldani,[3] Pierre Gounon,[5] Vittorio Ricci,[3] Mireille Cormont,[2] and Patrice Boquet[4]

[1]Unité 627 and [2]Unité 568, Institut National de la Santé et de la Recherche Medicale, Faculty of Medicine, 06107 Nice, Cedex 02, France
[3]Department of Experimental Medicine, Human Physiology Section, University of Pavia, 27100 Pavia, Italy
[4]Department of Clinical Bacteriology, Nice University Hospital, 06202 Nice, Cedex 03, France
[5]Centre Commun de Microscopie Appliquée, Faculté des Sciences, Université de Nice Sophia-Antipolis, 06108 Nice, Cedex 02, France

Glycosylphosphatidylinositol-anchored proteins (GPI-APs) are endocytosed by a clathrin-independent pathway into vesicles named GPI-AP–enriched early endosomal compartments (GEECs). We recently showed that the vacuolating toxin VacA secreted by *Helicobacter pylori* is endocytosed into the GEECs (Gauthier, N.C., P. Monzo, V. Kaddai, A. Doye, V. Ricci, and P. Boquet. 2005. *Mol. Biol. Cell.* 16:4852–4866). Unlike GPI-APs that are mostly recycled back to the plasma membrane, VacA reaches early endosomes (EEs) and then late endosomes (LEs), where vacuolation occurs.

In this study, we used VacA to study the trafficking pathway between GEECs and LEs. We found that VacA routing from GEECs to LEs required polymerized actin. During this trafficking, VacA was transferred from GEECs to EEs associated with polymerized actin structures. The CD2-associated protein (CD2AP), a docking protein implicated in intracellular trafficking, bridged the filamentous actin (F-actin) structures with EEs containing VacA. CD2AP regulated those F-actin structures and was required to transfer VacA from GEECs to LEs. These results demonstrate that sorting from GEECs to LEs requires dynamic F-actin structures on EEs.

Introduction

Bacterial protein toxins are useful probes to study endocytic mechanisms and intracellular trafficking pathways (Moya et al., 1985; Lord and Roberts, 1998; Falnes and Sandvig, 2000; Abrami et al., 2005). The *Helicobacter pylori* VacA toxin (M_r of 90 kD) is an important virulence factor of this bacterium involved in the induction of gastric ulcers and cancer (Blaser and Atherton, 2004). VacA is an A-B toxin that is transported from the cell surface to late endosomes (LEs), where it induces the

formation of large vacuoles. The toxin also escapes from its endocytic pathway to target mitochondria (Galmiche et al., 2000; Boquet et al., 2003; Blanke, 2005), but the precise mechanism of this event is still unknown.

We have recently determined the sequence of events that leads to the endocytosis and intracellular trafficking of VacA in HeLa and human adenocarcinoma gastric cells (see Fig. 1 A for schematic representation of the sequence; Gauthier et al., 2005). The toxin first binds to the cell surface on lipid rafts (Patel et al., 2002; Schraw et al., 2002; Gauthier et al., 2004). Binding of VacA occurs preferentially on lipid rafts clustered on membrane protrusions containing filamentous actin (F-actin) structures that are regulated by the Rac1 GTPase (Gauthier et al., 2005). Once bound to the cell surface, the toxin is rapidly internalized by a pinocytic mechanism that involves F-actin but is independent of clathrin, dynamin, and of the ARF6 GTPase. This pinocytic mechanism does not require tyrosine phosphorylation of cellular proteins and is not a macropinocytic process (Gauthier et al., 2005). VacA pinocytosis is regulated by the

Cdc42 GTPase activity (Gauthier et al., 2005), as shown for the internalization of non–cross-linked glycosylphosphatidyl-anchored proteins (GPI-APs; Sabharanjak et al., 2002). Accordingly, VacA is internalized into GPI-AP–enriched early endosomal compartments (GEECs) that have been recently described (Sabharanjak et al., 2002; Sharma et al., 2004; for review see Mayor and Riezman, 2004). In contrast to GPI-APs, which, upon pinocytosis into GEECs, are recycled to the plasma membrane via recycling endosomes (Sabharanjak et al., 2002), VacA is routed to early endosomes (EEs; EE antigen 1 [EEA1] positive; Birkeland and Stenmark, 2004) before reaching LEs (Gauthier et al., 2005).

To date, VacA is the only specific marker described for the GEEC–LE pathway. VacA-induced cell vacuolation occurring from LEs (Papini et al., 1994) is only slightly affected when microtubules are depolymerized (Papini et al., 1994; Li et al., 2004). This suggests that VacA intracellular trafficking toward LEs may be by a microtubule-independent process unlike that of receptor tyrosine kinases degraded into lysosomes (Gruenberg and Stenmark, 2004). Indeed, the transport of endocytosed molecules from sorting EEs to LEs is usually accomplished via endosomal carrier vesicles (also termed multivesicular bodies; Gruenberg and Stenmark, 2004) moving on microtubules by the use of molecular motors (Bomsel et al., 1990). Considering the specific pinocytic mechanism of VacA, we explored the possibility that this toxin may use a way other than microtubules to traffic from GEECs to LEs.

In this study, we examined whether VacA intracellular trafficking toward LEs is an actin-dependent process, with VacA transported through endosomal compartments associated with polymerized actin. We then tested whether VacA intracellular trafficking requires the adaptor molecule CD2-associated protein (CD2AP; Dustin et al., 1998; Kirsch et al., 1999), which is a good candidate to regulate the actin cytoskeleton and trafficking to LEs.

The interaction of CD2AP with actin (Lehtonen et al., 2002) and several actin-binding proteins (Badour et al., 2003; Hutchings et al., 2003; Lynch et al., 2003) favors a role for CD2AP in the dynamic actin remodeling process. This is also supported by its colocalization with the actin nucleation Arp2/3 complex and cortactin in actin dynamic-rich structures (leading edge of lamellipodia and comet tails; Schafer et al., 2000; Welsch et al., 2001, 2005). Moreover, upon CD2AP overexpression in COS-7 cells, an increase of F-actin patches surrounded by CD2AP together with a decrease in stress fibers has been observed (Kirsch et al., 1999; Badour et al., 2003).

Several pieces of evidence support a role for CD2AP in the regulation of trafficking to LEs. The interaction of CD2AP with Rab4 and c-Cbl was implicated in the trafficking between EEs and LEs (Cormont et al., 2003). In accordance with this observation, Lee et al. (2003) have shown that T cells isolated from CD2AP$^{-/-}$ mice failed to down-regulate the T cell receptor (TCR), although receptor internalization was not affected (Lee et al., 2003). Finally, electron microscopic analysis of podocytes from CD2AP haploinsufficient mice revealed defects in the formation of multivesicular bodies (Kim et al., 2003). The interaction of CD2AP with CAP-Z (capping protein of the Z line)

and cortactin, two actin-binding proteins, is involved in down-regulation of the activated TCR and EGF receptor, suggesting a link between receptor degradation and actin polymerization (Hutchings et al., 2003; Lynch et al., 2003). In the present study, we explore the function of CD2AP for the sorting of VacA from GEECs to LEs.

Results

VacA requires an intact actin cytoskeleton to be transferred from GEECs to LEs

We have previously unraveled the four steps of the endocytic process that drives VacA from the plasma membrane to LEs in HeLa cells, as depicted in Fig. 1 A (Gauthier et al., 2005). After binding to the cell by a Rac-dependent process (step 1) for 1 h at 4°C and upon warming to 37°C, VacA accumulates into GEECs within 10 min by a Cdc42-dependent nonmacropinocytic process (step 2), is enriched in the EEs within 30 min (step 3), and is transferred to LEs within 120 min (step 4).

The aim of this study is to examine whether the dynamics of the actin cytoskeleton are required for the transfer of VacA from GEECs (step 2) to EEs (step 3) and LEs (step 4). We first tested for a polymerized actin requirement in VacA intracellular trafficking in HeLa cells using actin poisons. After VacA binding at 4°C, cells were warmed for 30 min to allow the internalization of VacA into GEECs and EEs (Fig. 1 B). As shown previously, VacA molecules were colocalized with EEs, but a sizable portion of VacA was still associated with GEECs (Fig. 1 B and see Video 1 for 3D reconstructions; available at http://www.jcb.org/cgi/content/full/jcb.200609061/DC1). In a subsequent step, DMSO (for control), cytochalasin D (CD), or latrunculin B was added into the medium for the remaining 90 min required for the toxin to accumulate in LEs. In control cells, VacA was no longer associated with GEECs or EEs but colocalized with LEs (Fig. 1 C and see Video 2 for 3D reconstructions). It is worth noting that VacA induced a strong clustering of LEs (Fig. 1 C) as shown previously (Li et al., 2004). In contrast, in cells treated with actin poisons, a large portion of the pinocytosed VacA molecules did not reach LEs. Most of the internalized toxin molecules were found in GEECs based on cell peripheral localization of the toxin-labeled compartment and on the absence of EEA1 labeling associated with VacA (Fig. 1, D and E; and see Video 3 for 3D reconstructions). However, rare toxin molecules, which were probably already en route to LEs after 30 min of VacA pinocytosis, were found colocalized with lysosome-associated membrane protein 1 (LAMP1) compartments (Fig. 1, D and E).

We next determined whether the transport of VacA from GEECs to LEs requires polymerized actin using a functional toxin test. VacA-induced cell vacuolation occurs from LEs, and we have previously shown that the vacuolation process itself does not depend on F-actin (Ricci et al., 2000). Therefore, we investigated whether VacA-induced cell vacuolation was impaired by the addition of CD during the course of VacA internalization (Fig. 1 F). When VacA internalization was started in the presence of CD, cells did not develop vacuoles (Fig. 1 F). This confirms that pinocytosis of VacA is a strictly F-actin–dependent
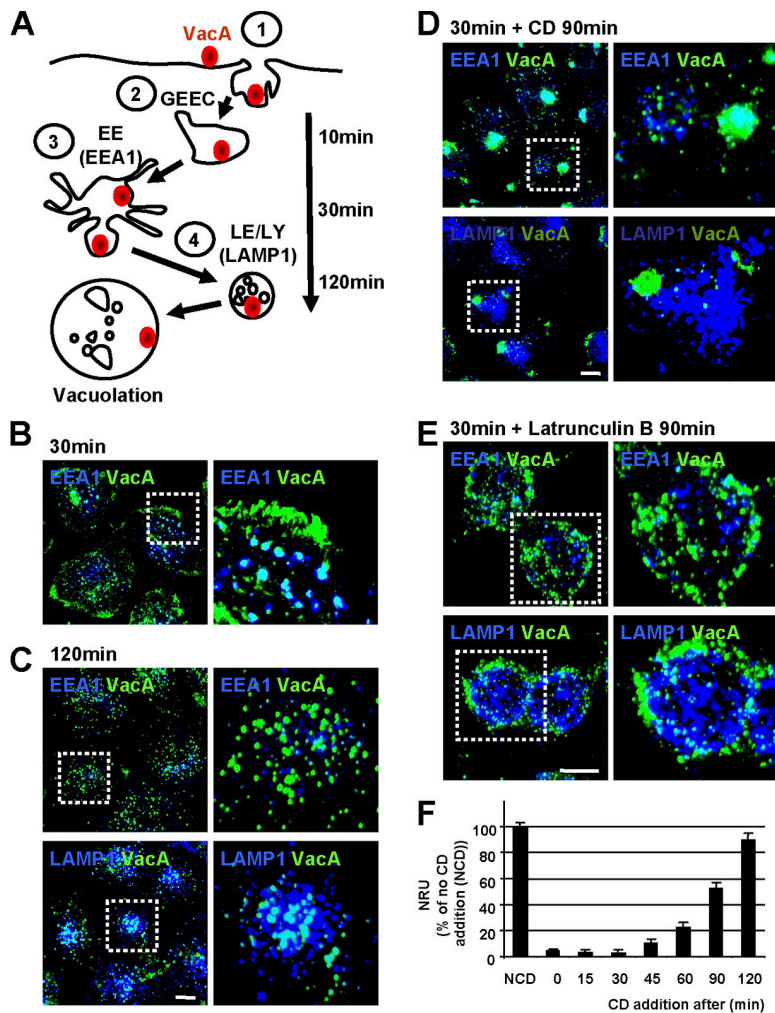
Figure 1. **Intracellular trafficking of VacA depends on F-actin.** (A) Model for the pinocytosis and intracellular trafficking of VacA as shown previously (Gauthier et al., 2005). (B and C) HeLa cells were intoxicated with VacA at 4°C for 1 h, washed, and incubated for 30 or 120 min at 37°C. Cells were then fixed, permeabilized, and processed for the detection of VacA (green), EEA1, or LAMP1 (blue) by indirect immunofluorescence. Cells were analyzed by confocal microscopy (see Videos 1 and 2 for 3D reconstructions; available at http://www.jcb.org/cgi/content/full/jcb.200609061/DC1). (D and E) Cells were incubated with VacA as in B and C, but, after the 30-min incubation period at 37°C, CD (D) or latrunculin B (E) was added to disrupt the actin cytoskeleton. Cells were further incubated for 90 min before being processed for the detection of VacA (green) and EEA1 or LAMP1 (blue; see Video 3 for 3D reconstructions). (B–E) Images on the right show enlarged views of the boxed regions in the corresponding left panels. All pictures present whole cell reconstructions from confocal sections and represent the merged images of the green (VacA) and blue (indicated endocytic markers) labeling. Bars, 10 μm. (F) HeLa cells were incubated at 4°C with VacA for 1 h and were washed and incubated at 37°C for a total period of 120 min. CD was added immediately or 15, 30, 45, 60, 90, or 120 min after the temperature shift. 5 mM NH_4Cl was added to the medium, and cells were incubated for a further 2 h to enable vacuolation to occur. Vacuolation was quantified by neutral red uptake (NRU). Error bars represent SD. NCD, no CD.

process (Ricci et al., 2000; Gauthier et al., 2004, 2005; Li et al., 2004). When CD was added 15 or 30 min after the beginning of VacA internalization, vacuolation was again not observed (Fig. 1 F), although VacA was already in GEECs and EEs (Fig. 1, A and B). When CD was added 45 min after the beginning of VacA pinocytosis, a small but definite vacuolation was observed (Fig. 1 F). The addition of CD at later times was progressively less and less efficient at blocking VacA-induced cell vacuolation. Together, these data support a model in which the transport of VacA from GEECs to LEs via EEs is dependent on polymerized actin.

VacA is transferred from GEECs to EEs associated with F-actin structures

Because the transport of VacA appears to depend on polymerized actin, we searched for the presence of F-actin structures associated with intracellular VacA-positive vesicles. VacA molecules internalized for 30 min were consistently present in vesicular compartments associated with F-actin structures (Fig. 2 A, insets 2–5). However, no polymerized actin structures were detected at the level of GEECs that still contained VacA (Fig. 2 A, inset 1). Polymerized actin structures associated with VacA-positive vesicles were localized most often in a polarized fashion onto the surface of the vesicles (Fig. 2 B and see Video 4 for

3D reconstructions; available at http://www.jcb.org/cgi/content/full/jcb.200609061/DC1), resembling the dynamic F-actin structures found on rocketing endosomes (Taunton et al., 2000). To ascertain that F-actin structures at the tip of VacA-containing endosomes could be observed in vivo and induced an actin-based motility of vesicles, we intoxicated GFP-actin–transfected HeLa cells with a fluorescent-tagged VacA (Cy5-VacA [VacA toxin labeled with Cy5 dye]). GFP-actin–transfected HeLa cells were incubated for 1 h with Cy5-VacA at 4°C, washed, incubated for 30 min at 37°C, and analyzed by confocal live cell microscopy. In these conditions, vesicles containing Cy5-VacA and harboring F-actin structures were easily observed (Figs. 2 C and S1). Furthermore, these structures were dynamically moving (Videos 5 and 6). To ascertain that vesicles containing VacA were moving by an actin-based motility mechanism, CD was added to Cy5-VacA–intoxicated HeLa cells after 20 min of endocytosis. As shown in Fig. S2, vesicles containing VacA had a threefold reduction of their motility in the presence of CD compared with the control preparation. This indicates that actin polymerization is required to efficiently propel VacA-containing endosomes.

We next analyzed the type of vesicles containing VacA that harbored F-actin structures using specific markers of EEs (EEA1) or LEs (LAMP1). 30 min after the onset of VacA

Figure 2. **VacA is transferred from GEECs to vesicular compartments harboring F-actin structures.** (A) HeLa cells were incubated with VacA at 4°C for 1 h and were washed and incubated for 30 min at 37°C. Cells were fixed, permeabilized, and processed for the detection of F-actin with FITC-phalloidin (green) and VacA (red) by indirect immunofluorescence. Cells were analyzed by confocal microscopy. One confocal section corresponding to each individual labeling and the merge images are shown. The numbered boxed areas delineate regions that are shown in the corresponding insets. The arrowhead points to a vesicle containing VacA, and the arrow indicates the F-actin structure associated to that vesicle. Bar, 10 μm. (B) Rotation (30° between each frame) in the Y plane of vesicles containing VacA associated with F-actin structures (see Video 4 for 3D reconstructions). (C) HeLa cells expressing GFP-actin were incubated with Cy5-VacA for 1 h at 4°C, washed, incubated for 30 min at 37°C, and recorded with a live confocal microscope at 1 frame/5 s as described in Materials and methods. Each frame represents one enlarged confocal section of Video 5 (also see Video 6 and Fig. S1; available at http://www.jcb.org/cgi/content/full/jcb.200609061/DC1).
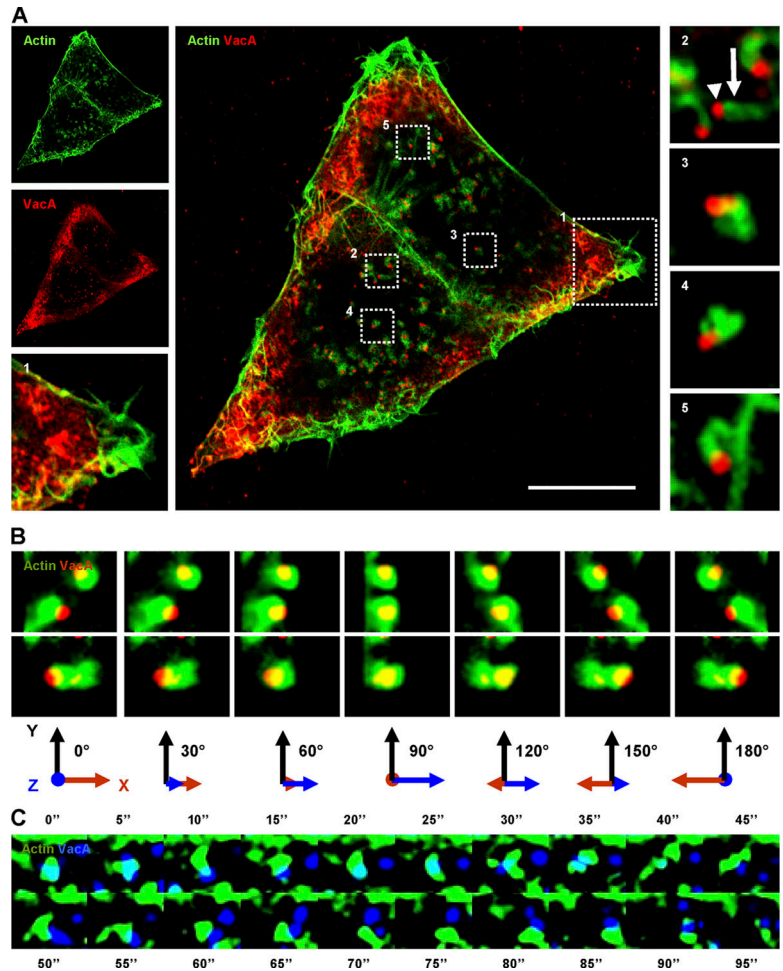
internalization, the vesicular compartments associated with F-actin stuctures and containing VacA were all labeled with EEA1 (Fig. 3 A; see Fig. S3 A for quantification and Video 7 for 3D reconstructions; available at http://www.jcb.org/cgi/content/full/jcb.200609061/DC1). LEs were clearly not associated with polymerized actin structures in these conditions (Fig. 3 B and see Fig. S3 A for quantification). We then investigated whether VacA was required for the formation of F-actin structures. As shown in Fig. 3 C, after 30 min of internalization, VacA was associated with fluorescent dextran (a marker of fluid-phase uptake) in EEs, indicating that GEECs are implicated in fluid-phase uptake as previously shown (Sabharanjak et al., 2002). Moreover, it has recently been shown that dextran is specifically taken up through a Cdc42-dependent mechanism like VacA (Cheng et al., 2006). In cells incubated with fluorescent dextran but without VacA, EEA1-positive vesicles containing dextran still exhibited polymerized actin structures at their tips (Fig. 3 D).

CD2AP is associated with F-actin structures on EEs containing VacA

CD2AP is a membrane-associated adaptor protein (Dustin et al., 1998; Kirsch et al., 1999) that has been implicated in the control of ligand intracellular trafficking toward the degradative pathway (Cormont et al., 2003; Kim et al., 2003; Kobayashi et al., 2004; Welsch et al., 2005). Importantly, CD2AP binds F-actin

(Lehtonen et al., 2002) and the Arp2/3 activator cortactin (Lynch et al., 2003). Therefore, we investigated whether CD2AP might be involved in VacA intracellular trafficking. We first investigated a possible colocalization between CD2AP and VacA. After 30 min of VacA endocytosis, both overexpressed and endogenous CD2AP were associated with VacA-containing vesicles (Fig. 4, A and B). Interestingly, CD2AP appeared to make a bridge between the surface of VacA-containing vesicles and the F-actin structures (Fig. 4 A). On the other hand, CD2AP was not detected in the GEECs that still contained VacA molecules (Fig. 4 A). Importantly, endogenous CD2AP and cortactin were colocalized (Fig. 4 C), suggesting that the two molecules could be involved in formation of the F-actin structures at the level of these intracellular vesicles.

CD2AP regulates the dynamics of F-actin structures at the tip of EEs

In light of our results, we next investigated whether CD2AP could be associated with dynamic F-actin structures in the cytosol. HeLa cells cotransfected with GFP-actin and DsRed-CD2AP but not treated with VacA were analyzed by live cell fluorescence microscopy. As shown in Fig. 5 A and in Video 8 (available at http://www.jcb.org/cgi/content/full/jcb.200609061/DC1), CD2AP was associated at the tip of F-actin structures that were moving randomly in the cytosol.
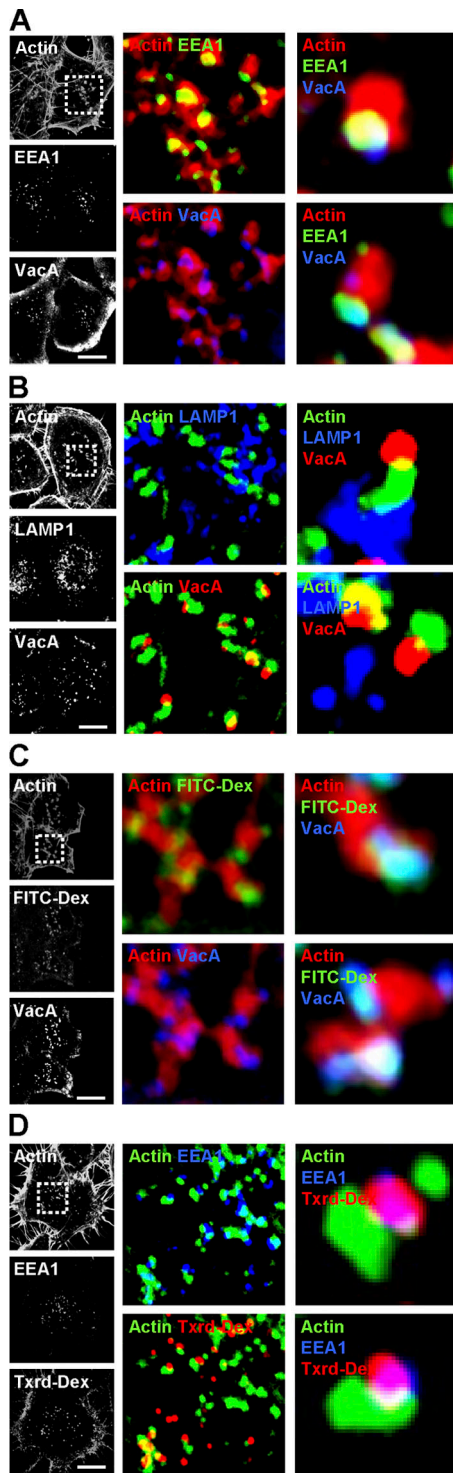
Figure 3. **Vesicles containing VacA or dextran and harboring actin tails are EEs.** (A and B) HeLa cells were incubated with VacA at 4°C for 1 h, washed, and incubated for 30 min at 37°C. Cells were fixed, permeabilized, and processed for labeling. A shows actin (red), EEA1 (green), and VacA (blue; see Video 7 for 3D reconstruction; available at http://www.jcb.org/cgi/content/full/jcb.200609061/DC1). B shows actin (green), LAMP1 (blue), and VacA (red). (C) HeLa cells were incubated with VacA at 4°C for 1 h and were washed and incubated for 30 min at 37°C in the presence of FITC-dextran (FITC-Dex). Cells were then processed for the detection of actin (red), FITC-dextran (green), and VacA (blue). (D) HeLa cells were incubated with Texas red–dextran (Txrd-Dex) and processed for the detection of actin (green), Texas red–dextran (red), and EEA1 (blue). (A–D) Cells were then analyzed by confocal microscopy.
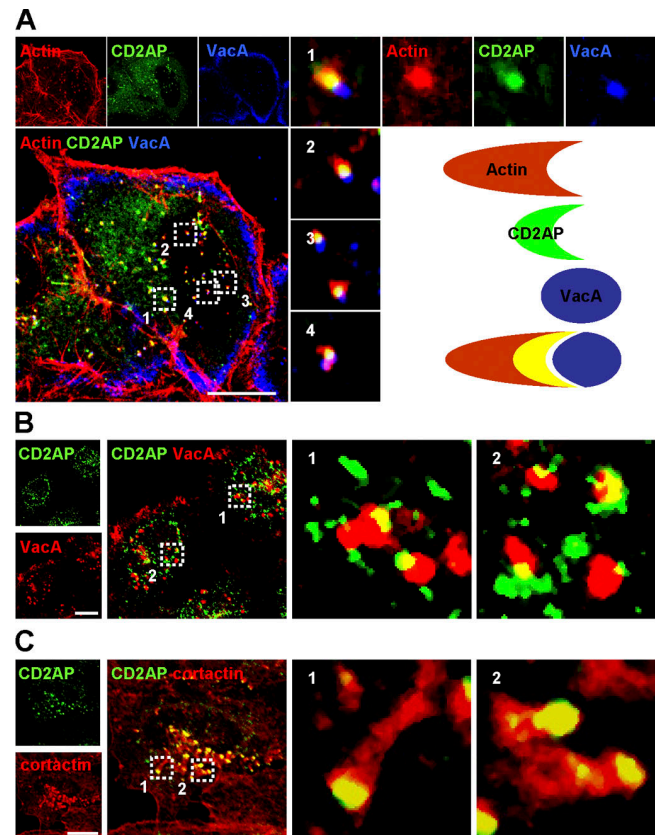

Figure 4. **CD2AP is located between VacA-containing EEs and the actin tail.** (A) HeLa cells expressing GFP-CD2AP (green) were incubated with VacA at 4°C for 1 h and were washed and incubated for 30 min at 37°C. Cells were fixed, permeabilized, and processed for the detection of actin (red) and VacA (blue). Cells were then analyzed by confocal microscopy. One confocal section corresponding to each individual labeling and a merge image are shown. The boxed areas delineate the regions that are shown in the corresponding insets. The scheme illustrates the respective localization of VacA, CD2AP, and actin deduced from the analysis of the merged images. As indicated, CD2AP is localized at the interface of the vesicle containing VacA and the F-actin tail (yellow and white). (B) HeLa cells were incubated with VacA at 4°C for 1 h and were washed and incubated for 30 min at 37°C. Cells were then processed for the detection of endogenous CD2AP (green) and VacA (red). (C) Untreated HeLa cells were processed for the detection of endogenous CD2AP (green) and cortactin (red). All pictures are from one single confocal section. Bars, 10 μm.

To study the possible role of CD2AP in formation of the dynamic actin structures, we looked for dominant-negative effects by expressing different domains of CD2AP (Monzo et al., 2005). From its N to C termini, CD2AP contains three SH3 domains, a proline-rich region, and a coiled-coil domain (Fig. 5 B; Dustin et al., 1998). Expression of full-length CD2AP in HeLa cells did not affect the formation of F-actin structures (Fig. 5, A and C). In contrast, expression of the first two SH3 domains of CD2AP (CD2AP-1–175) totally blocked the formation of F-actin structures compared with surrounding nontransfected cells, and the level of cortical F-actin was greater in transfected cells (Fig. 5 D). Expression of the C-terminal

One confocal section corresponding to each individual labeling is shown in black and white. The boxed areas delineate the enlarged merged regions. Bars, 10 μm.

Figure 5. **CD2AP regulates the formation of F-actin structures.** (A) HeLa cells expressing DsRed-CD2AP and GFP-actin were recorded at 1 frame/10 s as described in Materials and methods (see Video 8; available at http://www.jcb.org/cgi/content/full/jcb.200609061/DC1). The boxed areas indicate the fields of the video that are magnified in the four bottom panels showing, at four different times, the displacement of a vesicle labeled by fluorescent CD2AP (red) and its associated fluorescent F-actin structure (green). The arrows point to the CD2AP-labeled vesicles. (B) Structure of the GFP fusion proteins used: full-length CD2AP, the N-terminal part of CD2AP containing the first two SH3 domains of CD2AP (1–175), the C-terminal part of CD2AP containing the third SH3 domain, the proline-rich region and the coiled-coil domain of CD2AP (194–639), and the five tandem SH3 domains of intersectin (Inter-SH3). (C–F) HeLa cells expressing the different constructs (B) were incubated with VacA at 4°C for 1 h and were washed and incubated for 30 min at 37°C. Cells were fixed, permeabilized, and processed for the detection of actin (red) and the GFP-fused constructions (green). Cells were analyzed by confocal microscopy. One confocal section corresponding to each individual labeling and a merged image are shown. Boxed areas point to the transfected cells with the different GFP-CD2AP constructs (indicated on the left side of each panel) that are magnified to show the presence or absence of F-actin structures associated with VacA-containing vesicles (indicated by arrows). Arrows in insets show the presence or absence (1–175) of F-actin structures (see Video 9 for 3D reconstruction). Bars, 10 μm; (A, insets), 2 μm.
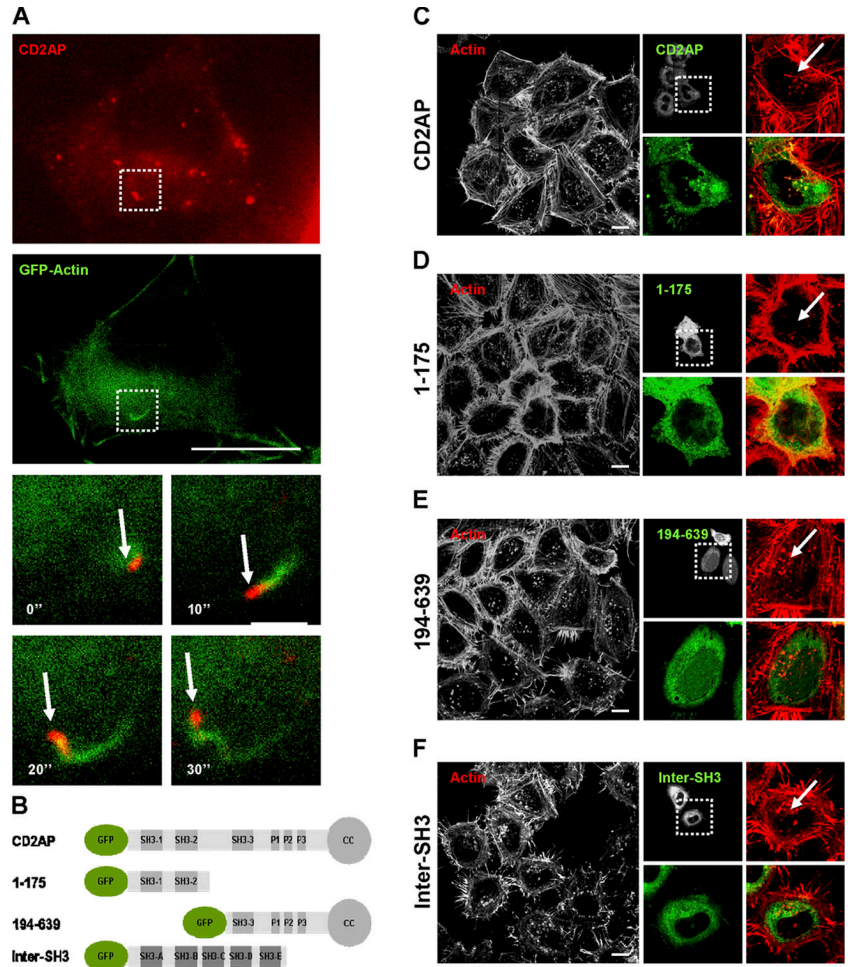
part of CD2AP (CD2AP-194–639) did not affect the formation of F-actin structures (Fig. 5 E; see Video 9 for 3D reconstructions of the effect of the three constructs and Fig. S3 B for quantifications; available at http://www.jcb.org/cgi/content/full/jcb.200609061/DC1). As a control for the specificity of the N-terminal domain of CD2AP, we expressed the SH3 domains of intersectin (Inter-SH3; Simpson et al., 1999). As shown in Fig. 5 F, the expression of Inter-SH3 did not block the formation of F-actin structures.

We next investigated the involvement of CD2AP in the formation of F-actin stuctures at the tips of EEs using an siRNA strategy that we have previously validated (Monzo et al., 2005). As shown in Fig. 6 A, the expression of CD2AP was decreased by nearly 90% in CD2AP-siRNA–treated HeLa cells. As observed in Fig. 6 B and Fig. S4 (available at http://www.jcb.org/cgi/content/full/jcb.200609061/DC1), CD2AP depletion led to a massive actin cytoskeleton remodeling with numerous stress fibers and a decrease in cortical actin labeling. These effects were not seen in cells transfected with control siRNA (Figs. 6 B and S4). Importantly, in the CD2AP-depleted cells, no F-actin structures were observed associated with EEA1-positive compartments still present in the cytosol (Figs. 6 B and S4). Altogether, these results indicate that the presence of F-actin structures on EEA1-positive EEs depends on CD2AP.

CD2AP-regulated F-actin structures are required to transfer VacA from GEECs to LEs

We next studied the role of CD2AP-regulated F-actin structures in the trafficking of VacA from GEECs to LEs. To this aim, we investigated the effects caused by overexpression of the different CD2AP constructs on the transfer of the toxin from GEECs to EEs (after 30 min of pinocytosis) and to LEs (after 120 min of pinocytosis). In GFP-CD2AP–transfected cells, 30 min after VacA pinocytosis, the toxin was found in GEECs and in F-actin structure-associated EEs (Fig. 7 A). In contrast, overexpression of the first two SH3 domains of CD2AP (CD2AP-1–175) led to an increased labeling of VacA in GEECs (Fig. 7, A [inset 2] and B). In these cells, VacA did not reach EEs compared with the nontransfected cells in the same field or with cells overexpressing Inter-SH3 (Fig. 7 B). Moreover, in the CD2AP-1–175-transfected cells, no vesicles associated with F-actin structures were observed at differences with the nontransfected cells or with the GFP-CD2AP–transfected cells (Fig. 7 A). Overexpression of the C-terminal part of CD2AP (CD2AP-194–639) did not lead to an increased labeling of VacA into GEECs, and all EEs containing VacA harbored F-actin structures at their tips (Fig. 7 A). Upon 120 min of pinocytosis, the expression of GFP-CD2AP did not affect the arrival of VacA into LEs (Fig. 7 C). In contrast, expression of the first two SH3 domains of CD2AP
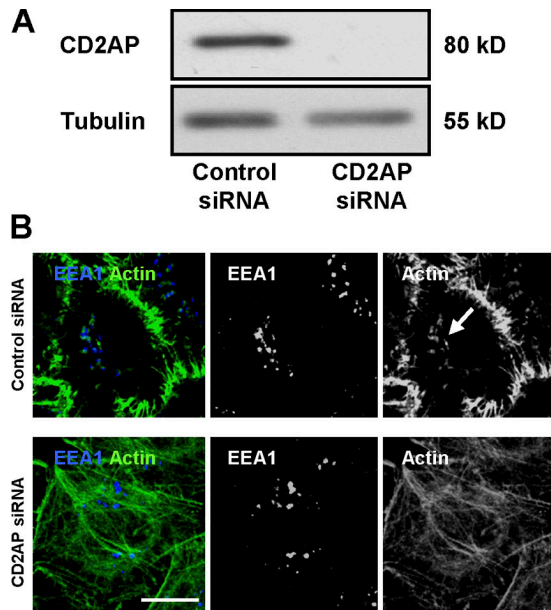
Figure 6. **CD2AP knockdown by siRNA leads to a loss of F-actin structures associated with EEs and to an increase of stress fibers.** (A) The expression of CD2AP was determined by Western blotting using cell extracts prepared 48 h after transfection with CD2AP siRNA or control siRNA. Western blotting against tubulin was used as loading control. (B) HeLa cells were fixed, permeabilized, and processed for the detection of actin (green) and EEA1 (blue) 48 h after transfection with CD2AP siRNA (bottom) or control siRNA (top). Cells were then analyzed by confocal microscopy. One confocal section corresponding to each individual labeling and a merged image are shown (see Fig. S4 for a full field of analyzed cells and confocal z stack of cells from B; available at http://www.jcb.org/cgi/content/full/jcb.200609061/DC1). Arrow shows the presence of actin tails in the control. Bar, 10 μm.

(CD2AP-1–175) blocked the arrival of VacA into LEs, and VacA remained associated with GEECs (Fig. 7 C). Expression of either the C-terminal part of CD2AP or of Inter-SH3 did not impair the arrival of VacA into LEs (Fig. 7 C).

To further explore the role of CD2AP in VacA transport from GEECs to LEs, we studied whether VacA-induced cell vacuolation was affected in cells overexpressing CD2AP or truncated forms of that protein. The toxin-induced vacuolation of cells overexpressing the different CD2AP constructs was followed by videomicroscopy (Fig. 8 and Video 10; available at http://www.jcb.org/cgi/content/full/jcb.200609061/DC1), and the number of vacuolating cells was quantified (Fig. 8 B). Only the expression of CD2AP-1–175 was able to produce a substantial decrease in the formation of toxin-induced large vacuoles in cells (Fig. 8 and Video 10).

To definitively establish the role of CD2AP in the intracellular trafficking of VacA toward LEs, we depleted HeLa cells of CD2AP using siRNA. In CD2AP-depleted cells, after 120 min of VacA endocytosis, the toxin did not reach LEs as it did in cells treated with the control siRNA. Instead, VacA remained within the GEEC (Fig. 9 A). Furthermore, the formation of toxin-induced large vacuoles was inhibited by 50% in CD2AP-depleted cells (Fig. 9, B and C).

We verified that CD2AP depletion did not affect the pinocytosis of VacA using a biochemical assay (Fig. 9, D and E). Cells were treated with proteinase K to degrade
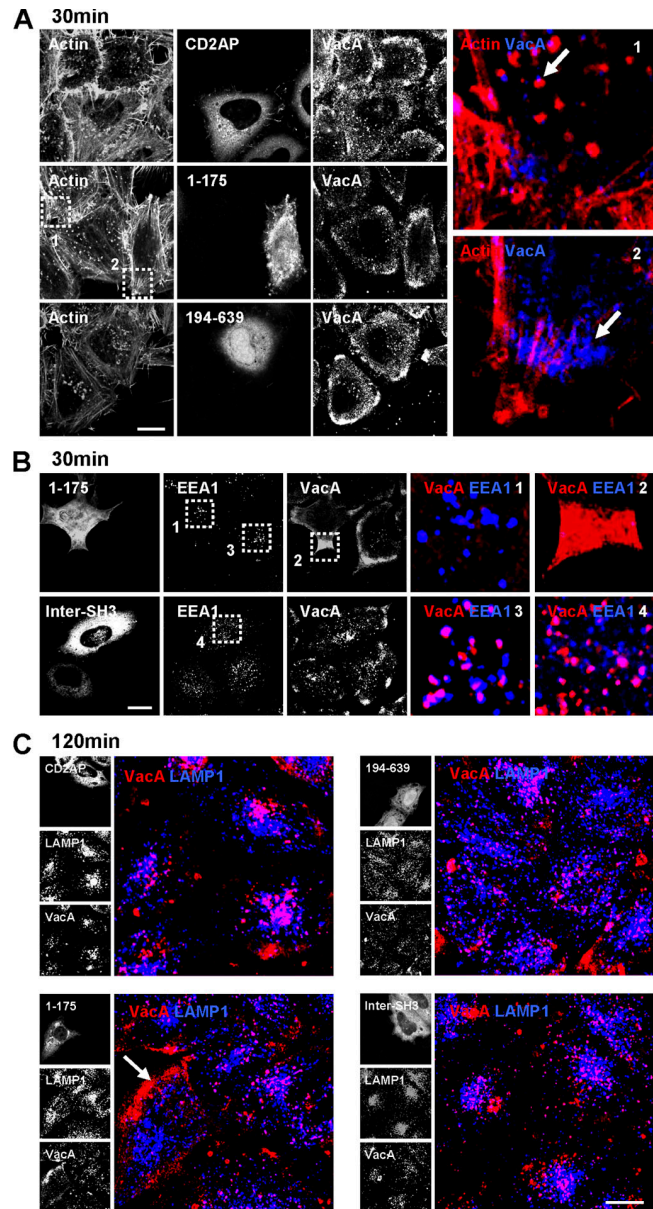

Figure 7. **Expression of the first two SH3 domains of CD2AP blocks the transfer of VacA from GEECs to the LEs.** (A) HeLa cells transfected with CD2AP, CD2AP-1–175, and CD2AP-194–639 were incubated with VacA at 4°C for 1 h and were washed and incubated for 30 min at 37°C. Cells were fixed, permeabilized, and processed for the detection of actin, VacA, and the different constructs. Cells were analyzed by confocal microscopy. One confocal section corresponding to each individual labeling are shown in black and white. Insets represent merges between VacA labeling (blue) and actin labeling (red) in nontransfected (1) or CD2AP-1–175-transfected cells (2). The arrows point to VacA-containing vesicles associated with an F-actin structure. (B) Same conditions as in A, but HeLa cells were transfected with CD2AP-1–175 or Inter-SH3, and EEs were detected with EEA1 antibody. Insets represent merges between VacA labeling (red) and EEA1 labeling (blue) in a nontransfected cell (3), in a CD2AP-1–175-transfected cell with VacA present in the GEECs (2) and nondetectable in the EEs (1), and in an Inter-SH3–transfected cell (4). (A and B) The boxed areas delineate the regions that are enlarged. (C) Same conditions as in A or B, but HeLa cells were incubated for 120 min at 37°C, and LEs were detected with LAMP1 antibody. In the merge images, VacA is shown in red, and LAMP1 is shown in blue. In CD2AP-1–175-transfected cells, VacA is enriched in GEECs (arrow) and is not found in LEs compared with adjacent nontransfected cells or with cells that have been transfected with the other constructs. Bars, 10 μm.
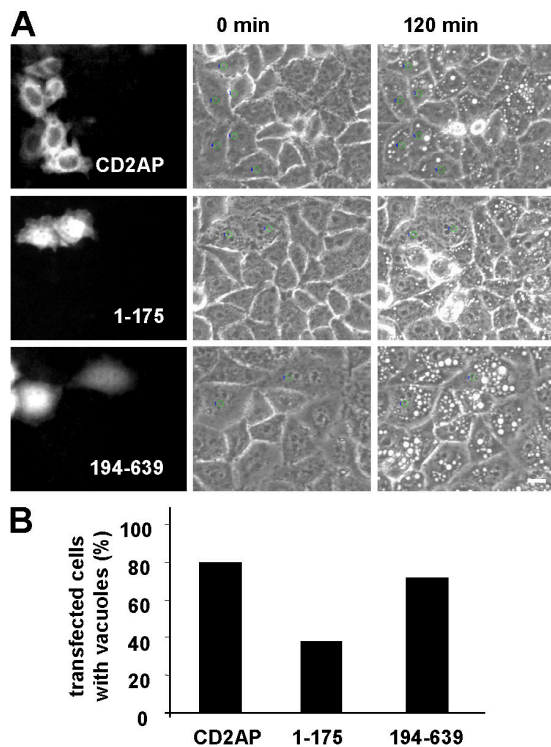
Figure 8. Expression of the first two SH3 domains of CD2AP inhibits the vacuolation of LEs induced by VacA. (A) HeLa cells transfected with CD2AP, CD2AP-1–175, and CD2AP-194–639 were incubated with VacA at 4°C for 1 h and were washed and analyzed by videomicroscopy for 120 min at 37°C in DME medium containing 5 mM NH₄Cl. Vacuolation was followed in transfected cells. (B) Transfected cells that developed vacuoles were quantified. At least 50 transfected cells were analyzed for each condition (Video 10, available at http://www.jcb.org/content/full/jcb .200609061/DC1). Bar, 10 μm.

extracellular VacA. The amount of remaining VacA corresponding to the toxin that has been internalized was determined by Western blotting. As a control, cells were treated with CD to block VacA pinocytosis as described previously (Gauthier et al., 2005). Although CD totally blocked the pinocytosis of VacA (Fig. 9 E), no difference in the amounts of pinocytosed VacA between siRNA control and siRNA CD2AP–treated cells was observed (Fig. 9 D). Collectively, these results show that CD2AP is implicated in the sorting and transport of VacA from GEECs to LEs by regulating the formation of F-actin structures at the tip of EEs.

Discussion

GPI-APs are endocytosed by a clathrin-independent pathway and accumulate into early endosomal compartments named GEECs (for review see Mayor and Riezman, 2004). We recently showed that the vacuolating VacA toxin associates with lipid rafts and is pinocytosed into GEECs (Gauthier et al., 2005). Subsequently, unlike GPI-APs that are recycled back to the plasma membrane, VacA is sorted to EEs. However, it was demonstrated very recently that GPI-APs, like VacA, are transferred from GEECs to EEs (Kalia et al., 2006). VacA is subsequently transported from EEs to LEs. There, VacA induces the

clustering (Li et al., 2004) and swelling of LEs, leading to the formation of large vacuoles (Papini et al., 1994). To date, VacA is the only specific marker described for the GEEC–LE pathway. Therefore, we used VacA as a tool to study this trafficking pathway. Importantly, we show that this trafficking is dependent on polymerized actin. Indeed, disrupting the actin cytoskeleton by means of specific drugs led to the accumulation of VacA into GEECs and to inhibition of the vacuolation induced by the toxin. We found that F-actin structures are formed on EEs and are required for the trafficking of VacA from GEECs to LEs. The actin regulator CD2AP controls those actin structures on EEs. Indeed, disrupting CD2AP function by either overexpressing truncated CD2AP or by specific depletion using siRNA led to a loss of the F-actin structures on EEs, resulting in the accumulation of VacA in GEECs. The accumulation of VacA in GEECs suggests that GEECs are linked to EEs and that dynamic F-actin structures on EEs help to sort molecules to reach LEs.

Presence of F-actin structures on EEA1 vesicles containing VacA

Dynamic F-actin structures were first described as being associated with bacterial pathogens such as *Listeria monocytogenes* or *Shigella flexneri*, which, upon internalization into the cell, induce the polymerization of host actin on their surface (Welch and Mullins, 2002). Since then, several studies have found that endogenous F-actin structures in mammalian cells at the level of the plasma membrane help the invagination and departure of vesicles from the plasma membrane (Engqvist-Goldstein and Drubin, 2003; Kaksonen et al., 2005). In macrophages, for example, it has been shown that dextran-containing vesicles were associated with actin tails that bring the vesicle away from the plasma membrane during internalization (Merrifield et al., 1999). There are few examples of endogenous F-actin tails at the level of trafficking endosomes. The presence of F-actin tails at the level of Golgi vesicles, which is required for Golgi to LE trafficking or for the delivery of raft-associated proteins from the Golgi to the apical membrane of polarized cells, was demonstrated (Carreno et al., 2004; Guerriero et al., 2006). Moreover, Morel et al. (Morel, E., N. Mayran, and J. Gruenberg. 2004. Proceedings of the 2004 European Laboratory Science Organisation Meeting. Abstr. E124.) suggested that polymerized actin was present on EEs in HeLa cells. The occurrence of F-actin structures associated on intracellular compartments was first described on purified HeLa cell endosomes in an in vitro system using *Xenopus laevis* oocyte extract (Taunton et al., 2000). In this system, EEs and LEs, which are defined by the presence of transferrin and LAMP1, respectively, were highly motile and propelled by dynamic F-actin tails (Taunton et al., 2000). In the present study, we have been able to detect F-actin structures in the cells, mostly on EEA1 endosomes containing VacA or dextran but not on LEs. The absence of F-actin structures on LEs is in accordance with the results of Carreno et al. (2004). The difference between our results and those obtained from the in vitro system using *Xenopus* oocyte extract (Taunton et al., 2000) could be the result of the presence of regulators that inhibit the formation of F-actin structures on LEs in
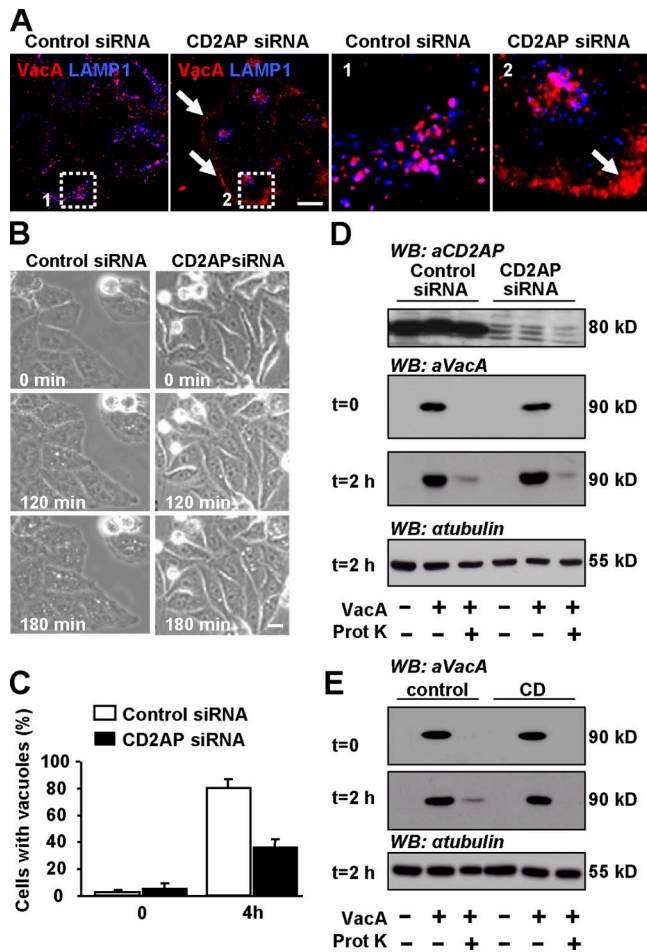
Figure 9. Down-regulation of CD2AP expression inhibits VacA transfer from GEECs to LEs and VacA-induced vacuolation. (A) 36 h after transfection with control siRNA (left) or CD2AP siRNA (right), HeLa cells were incubated with VacA at 4°C for 1 h, washed, and incubated for 120 min at 37°C. Cells were fixed, permeabilized, and processed for the detection of VacA and LAMP1. Cells were then analyzed by confocal microscopy. Pictures and insets represent the merge between VacA labeling (red) and LAMP1 labeling (blue) from single confocal sections. The boxed areas delineate the regions that are enlarged in the corresponding insets. The arrows show that upon CD2AP depletion, VacA remains in the GEECs. (B) Cells were transfected with control siRNA or CD2AP siRNA. 36 h later, they were incubated at 4°C for 1 h with VacA, washed, and incubated at 37°C for 4 h with DME containing 5 mM NH₄Cl. Cells were analyzed by videomicroscopy. (C) Vacuolating cells were scored at the beginning of the film (0) and 4 h later. Results are expressed as the percentage of vacuolating cells among the entire cell population and represent the means ± SEM (error bars) of three independent videos. (D) The amount of intracellular (proteinase K resistant) VacA is identical in cells expressing or not expressing CD2AP. HeLa cells were transfected with control or CD2AP siRNA as described in Materials and methods. 3 d later, cells were treated with VacA at 4°C for 1 h (t = 0), and internalization of VacA was allowed for 2 h at 37°C (t = 2 h). Cells were then treated with proteinase K as described in Materials and methods to degrade extracellular VacA. The amount of intracellular VacA (i.e., proteinase K resistant) is identical in cells expressing or not expressing CD2AP, indicating that VacA internalization occurs independently of CD2AP. Western blotting against tubulin was used as loading control for the 2-h time point. (E) As a control, cells were pretreated with CD to block VacA pinocytosis as described previously (Gauthier et al., 2005). HeLa cells were pretreated or not pretreated with CD for 20 min before VacA binding and were processed as in D. Bars, 10 μm.

the cell. On the other hand, F-actin structures on LEs may exist in our system but are too transient to be detected readily.

VacA causes apoptosis by targeting the mitochondria and inducing the release of cytochrome *c* (Galmiche et al., 2000). It has been previously shown that organelle to organelle contact between iron-containing EEs and mitochondria likely replenishes mitochondrial iron by direct transfer (Zhang et al., 2005). It has also been observed that *L. monocytogenes* moving intracellularly by an F-actin–based motility frequently collides with mitochondria (Lacayo and Theriot, 2004). We propose that VacA could exploit EEs exhibiting dynamic F-actin motility as a route to achieve a direct transfer to mitochondria.

CD2AP regulates F-actin structures on EEs

Our observation that VacA-containing EEs were associated with F-actin structures prompted us to search for the presence of molecules known to be involved in this process. CD2AP has been shown to be involved in the endocytic degradative pathway and in actin remodeling processes and was therefore a prime candidate (Dikic, 2002). From our present results, it appears that CD2AP bridges the surface of VacA-containing vesicles and the F-actin structures. This is in accordance with the work of Schafer et al., (2000), who observed CD2AP at the head of F-actin tails in Ptk1 cells overexpressing Arf6.

Upon CD2AP overexpression, some groups have observed an increase of F-actin patches surrounded by CD2AP together with a decrease in stress fibers (Kirsch et al., 1999; Badour et al., 2003). These F-actin patches likely correspond to F-actin structures that we have observed associated with EEs. Accordingly, in transfected cells strongly overexpressing full-length CD2AP, we observed an increase of polymerized actin surrounding VacA-containing EEA1 vesicles and overlapping the CD2AP labeling (unpublished data). We also found that CD2AP depletion led to an increase in actin stress fibers and to the depletion of F-actin structures on EEs that were still observed in the cytosol.

The role of CD2AP in the regulation of F-actin structures is probably related to its interaction with actin and actin-binding proteins. Indeed, CD2AP binds directly to actin (Lehtonen et al., 2002) and to three actin regulators, CAP-Z, cortactin, and WASP (Wiscott-Aldrich syndrome protein), via PSTPIP1 (Badour et al., 2003; Hutchings et al., 2003; Lynch et al., 2003). CAP-Z and cortactin have been implicated in similar processes (for example, the formation of F-actin tails; Welch and Mullins, 2002). Accordingly, we found that endogenous CD2AP is associated with cortactin. This is in agreement with the work of Welsch et al. (2001) showing that CD2AP is colocalized on F-actin patches together with cortactin and Arp2/3 in podocytes. Moreover, CD2AP could bind to another adaptor protein called Alix/AIP1 (Chen et al., 2000; Kurakin et al., 2003), a protein that has been shown recently to be a regulator of actin on EEs (Cabezas et al., 2005). Alix depletion using siRNA leads to an increase of actin reticulation around EEs (Cabezas et al., 2005). These results suggest that CD2AP and Alix could work as positive and negative regulators of actin recruitment on the EEs, respectively.

CD2AP regulates VacA traffic between GEECs and LEs

In this study, we found that CD2AP was involved in the trafficking of VacA from GEECs to LEs, which is in line with the role of CD2AP in the degradative pathway observed in podocytes (Kim et al., 2003) and for TCR intracellular trafficking (Lee et al., 2003). Upon CD2AP depletion or overexpression of the dominant-negative mutant, VacA was confined to GEECs, and no other cytosolic compartment was found to contain VacA. This suggests that EEs containing VacA are endocytic structures that connect GEECs to LEs likely through a process involving EE motility. Several possibilities may explain the role of EEs harboring F-actin structures in the transport of ligands from GEECs to LEs.

Our model is that EEs with a CD2AP-containing F-actin structure represent a specific population of EEs issued from GEECs that mature and directly connect to this pinocytic compartment to LEs. In support of this model, Kim et al. (2003) have shown that there is failure in the formation of multivesicular bodies in CD2AP$^{+/-}$ podocytes, impairing the transport of pinocytosed ligands to lysosomes. More recently, it was shown that in podocytes, CD2AP was associated with dextran-loaded vesicles labeled with Rab4 and harboring dynamic F-actin structures. These compartments are highly motile in the cytosol (Welsch et al., 2005). Blockage of ligands en route to lysosomes in the CD2AP knockout animals has been confirmed in T cells in which the signal persistence upon TCR activation is caused by a decrease in the TCR degradation. Indeed, TCR is not found in lysosomes in CD2AP knockout cells (Lee et al., 2003). Clearly, this was not caused by the inhibition of TCR internalization but by inhibition of the trafficking toward the lysosomes (Lee et al., 2003). Furthermore, we have previously shown that CD2AP was involved in the intracellular trafficking between EEs and LEs (Cormont et al., 2003). We have found that the co-expression of CD2AP with Rab4 leads to an enlargement of endosomes containing both EE markers such as EEA1 and LE markers such as Rab7 (Cormont et al., 2003).

Another possibility that we cannot exclude is that VacA in specific EEA1 compartments endowed with an F-actin–dependent motility regulated by CD2AP might rapidly mix with Rab5-sorting endosomes receiving their content mainly from the clathrin pathway. This would allow the transfer of their ligands to LEs by either endosomal carrier vesicles/multivesicular bodies (Gruenberg and Stenmark, 2004) or by a maturation process (Rink et al., 2005).

From our observations, it appears that VacA and CD2AP could delineate an intracellular pathway for the degradation of raft-associated components like the TCR (Miceli et al., 2001). Interestingly, it has been shown that during cell division, the midbody contains rafted components (Ng et al., 2005). We have previously shown that CD2AP is involved in midbody scission (Monzo et al., 2005). During the late step of cytokinesis, endocytosis/pinocytosis of rafted components could be achieved through the formation of F-actin structures under the membrane of the midbody.

We did not find any modification of VacA internalization in CD2AP siRNA–treated cells as observed for TCR in CD2AP knockout cells (Lee et al., 2003). The overexpression of mutant forms of CD2AP has implicated CD2AP in the internalization of several growth factor receptors. In particular, overexpression of the N-terminal part of CD2AP containing the SH3 domains leads to the inhibition of growth factor receptor internalization (Kobayashi et al., 2004). This effect is probably responsible for the actin phenotype observed in our experiments. Indeed, upon overexpression of the two first SH3 domains of CD2AP, we observed an increase in cortical actin accompanied by the loss of F-actin structures. This increase in cortical actin is probably a consequence of increased growth factor receptor signaling, as the receptors are probably still associated with the plasma membrane. Surprisingly, we did not observe any effect of CD2AP depletion on EGF receptor endocytosis (unpublished data). This indicates that the effect of SH3 domain overexpression is probably the result of the inhibition of another SH3-containing protein or that another protein rescues CD2AP in its receptor internalization function. CD2AP belongs to the same family as the adaptor molecule CIN85 (Dikic, 2002), which is also involved in receptor internalization (Petrelli et al., 2002; Soubeyran et al., 2002). The homology between the two adaptor proteins is greatest in the N-terminal region, suggesting that overexpression of the first two CD2AP SH3 domains would also interfere with CIN85 function. Because the function of CD2AP on F-actin structures is not rescued, it appears that the two proteins do not share all of their functions in mammalian cells.

Materials and methods

Cell lines, bacterial strains, plasmids, toxins, and antibodies

HeLa cells (from human cervical carcinoma; a gift of T.L. Cover, Vanderbilt University, Nashville, TN) were cultured and transfected as previously described (Ricci et al., 2000; Monzo et al., 2005). Full-length CD2AP cDNA (Cormont et al., 2003) as well as sequences encoding for the truncated forms of CD2AP were amplified by PCR and subcloned into pEGFP-C1 or into pDsRed-C1 expression plasmids (BD Biosciences and CLONTECH Laboratories, Inc.) in frame with the sequence encoding GFP or DsRed. pEGFP–CD2AP-1–175 was obtained using site-directed mutagenesis as described previously (Monzo et al., 2005). The five tandem SH3 domains of intersectin tagged with GFP (Simpson et al., 1999) were provided by P.S. McPherson (McGill University, Montreal, Canada). VacA was purified from the *H. pylori* 60190 strain (49503; American Type Culture Collection) according to Cover and Blaser (1992). Immediately before use on cells, purified VacA (2 μg/ml in all experiments) was acid activated as described previously (de Bernard et al., 1995). Rabbit polyclonal IgG 958 anti-VacA and -VacA mAbs were gifts from T.L. Cover (Garner and Cover, 1996). Polyclonal anti-CD2AP antibodies were purchased from Santa Cruz Biotechnology, Inc. Anticortactin mAb was obtained from Upstate Biotechnology. Anti–tubulin mAb was obtained from Sigma-Aldrich. Anti-EEA1 and -LAMP1 mAbs were purchased from BD Biosciences. Texas red– and Cy5-labeled secondary antibodies against rabbit IgG were purchased from Invitrogen, and anti–mouse secondary antibodies labeled with FITC or Cy5 were obtained from DakoCytomation. Phalloidin-FITC and -TRITC were purchased from Sigma-Aldrich, and Texas red–coupled phalloidin and Texas red–labeled or FITC-labeled 70-kD dextran were obtained from Invitrogen. VacA toxin was labeled with Cy5 dye by incubation in borate buffer, pH 8.5, and labeled VacA was separated from unconjugated dye by gel filtration and eluted in PBS. Cy5-VacA was stored in melting ice and alkali activated (Yahiro et al., 1999) by drop-wise addition of 0.4 N NaOH immediately before use. To rule out the possibility that the labeling procedure may alter the biological behavior of the toxin, both the vacuolating activity and the intracellular trafficking of Cy5-VacA was compared with those of the native toxin (Fig. S5, available at http://www.jcb.org/cgi/content/full/jcb.2006090651/DC1).

Fixation, immunofluorescence, and microscopy
Immunofluorescence studies and analysis by confocal microscopy were performed as previously described (Ricci et al., 2000; Gauthier et al., 2004) using a PL APO 63× NA 1.40 oil objective (TCS SP; Leica). The images were combined and merged using Photoshop software (Adobe). For endogenous CD2AP labeling, cells were fixed with methanol rather than PFA as described previously (Monzo et al., 2005). For LAMP1 detection, 0.1% Triton X-100 in the permeabilization buffer was replaced by 0.1% saponin. For 2D deconvolution or 3D reconstructions, fluorescence signals were recorded using a microscope (Axiovert 200; Carl Zeiss MicroImaging, Inc.) equipped with a shutter-controlled illumination system (HB0100 with Fluo Arc; Carl Zeiss MicroImaging, Inc.) and a cooled digital CCD camera (CoolSnap HQ; Roper Scientific). Images were reconstructed using MetaMorph 2.0 image analysis software (Universal Imaging Corp.) and QuickTime Pro 5 (Apple). For 3D reconstructions using confocal sections, ImageJ software was used (National Institutes of Health; http://rsb.info.nih.gov/ij/). Studies of VacA endocytosis were performed as previously described (Gauthier et al., 2005). In brief, VacA was first incubated with cells for 1 h at 4°C. After three washes in cold DME, cells were transferred to DMSO-DME, cytochalasin-DME, or latrunculin B–DME prewarmed to 37°C and incubated at 37°C for the times indicated in the figure legends before being processed for immunofluorescence analysis. CD (Sigma-Aldrich) and latrunculin B (Sigma-Aldrich) were used at 20 μM. The fluid-phase marker Texas red–labeled 70-kD dextran was used as previously described (Gauthier et al., 2005). Quantification of colocalization was performed using the cell counter plugin in ImageJ.

Cell vacuolation experiments
VacA-induced cell vacuolation and quantification of the degree of cell vacuolation by means of neutral red dye uptake assay were performed as previously described (Ricci et al., 2000).

Depletion of CD2AP by RNA interference (siRNA)
HeLa cells (40–50% confluent) cultivated in DME containing 10% FCS in 35-mm-diameter dishes were transfected with siRNA directed against CD2AP (Santa Cruz Biotechnology, Inc.) or a scramble siRNA (Eurogentec) using Oligofectamine (Invitrogen) as previously described (Monzo et al., 2005). Depletion of CD2AP expression was determined by Western blotting.

Time-lapse imaging
Cells were filmed under constant conditions (5% CO_2 at 37°C) with a motorized microscope (Axiovert 200; Carl Zeiss MicroImaging, Inc.) and a cooled digital CCD camera (CoolSnap HQ; Roper Scientific) and were observed by fluorescent or phase-contrast optics (LP Achroplan phase 2 20× NA 0.40 and plan-NEOFLUAR 40× NA 1.3 objectives lenses). Images were recorded and processed using MetaMorph 2.0 and QuickTime Pro5.

Proteinase K treatment
HeLa cells pretreated with CD or transfected with siRNA were incubated with activated VacA at 4°C for 1 h, washed, and incubated for 2 h at 37°C to induce the internalization of VacA (t = 2 h). At the end of the incubations, cells were treated or not treated with 1 μg/ml proteinase K (Sigma-Aldrich) for 30 min at 4°C to degrade extracellular VacA. Cells were then washed extensively with medium containing 2 mM PMSF, 20% BSA, and 20% FCS to block the activity of proteinase K and then with medium containing 2 mM PMSF. Cells were scrapped in Laemmli buffer, and the amount of intracellular VacA (i.e., proteinase K resistant) was determined by Western blotting with a specific antibody.

Online supplemental material
Fig. S1 shows the two cells from which two enlarged regions are presented in Video 5. Fig. S2 shows that treatment of cells by CD inhibits the motility of VacA-containing vesicles. Fig. S3 presents some quantifications of F-actin structures. Fig. S4 shows full fields of cells and some sequential confocal sections from the bottom to the top of the cells selected in Fig. 6 B. Fig. S5 shows that the Cy5-VacA toxin has intracellular trafficking and vacuolating activity identical to that of the native cytotoxin. Videos 1, 2, and 3 are 360° rotations of 3D reconstructed HeLa cells presented in Fig. 1 B, Fig. 1 C, and Fig. 1 E, respectively. Video 4 is a 360° rotation of a 3D reconstructed part of a HeLa cell processed as described in Fig. 2. Video 5 shows that vesicles containing VacA exhibit F-actin structures and move rapidly in the cytosol. Video 6 shows a specific field of Video 5 focusing on the motility of a VacA-containing vesicle associated with an F-actin structure.

Video 7 is a 360° rotation of a 3D reconstructed HeLa cell processed as described in Fig. 3 A. Video 8 shows that CD2AP is associated with dynamic F-actin structures. Video 9 is a 360° rotation of 3D-reconstructed HeLa cells processed as described in Fig. 5 (C–E). Video 10 shows that expression of the first two SH3 domains of CD2AP inhibits the vacuolation of LEs induced by VacA. Online supplemental material is available at http://www.jcb.org/cgi/content/full/jcb.200609061/DC1.

References

Abrami, L., N. Reig, and F.G. van der Goot. 2005. Anthrax toxin: the long and winding road that leads to the kill. *Trends Microbiol.* 13:72–78.

Badour, K., J. Zhang, F. Shi, M.K. McGavin, V. Rampersad, L.A. Hardy, D. Field, and K.A. Siminovitch. 2003. The Wiskott-Aldrich syndrome protein acts downstream of CD2 and the CD2AP and PSTPIP1 adaptors to promote formation of the immunological synapse. *Immunity.* 18:141–154.

Birkeland, H.C., and H. Stenmark. 2004. Protein targeting to endosomes and phagosomes via FYVE and PX domains. *Curr. Top. Microbiol. Immunol.* 282:89–115.

Blanke, S.R. 2005. Micro-managing the executioner: pathogen targeting of mitochondria. *Trends Microbiol.* 13:64–71.

Blaser, M.J., and J.C. Atherton. 2004. *Helicobacter pylori* persistence: biology and disease. *J. Clin. Invest.* 113:321–333.

Bomsel, M., R. Parton, S.A. Kuznetsov, T.A. Schroer, and J. Gruenberg. 1990. Microtubule- and motor-dependent fusion in vitro between apical and basolateral endocytic vesicles from MDCK cells. *Cell.* 62:719–731.

Boquet, P., V. Ricci, A. Galmiche, and N.C. Gauthier. 2003. Gastric cell apoptosis and *H. pylori*: has the main function of VacA finally been identified? *Trends Microbiol.* 11:410–413.

Cabezas, A., K.G. Bache, A. Brech, and H. Stenmark. 2005. Alix regulates cortical actin and the spatial distribution of endosomes. *J. Cell Sci.* 118:2625–2635.

Carreno, S., A.E. Engqvist-Goldstein, C.X. Zhang, K.L. McDonald, and D.G. Drubin. 2004. Actin dynamics coupled to clathrin-coated vesicle formation at the trans-Golgi network. *J. Cell Biol.* 165:781–788.

Chen, B., S.C. Borinstein, J. Gillis, V.W. Sykes, and O. Bogler. 2000. The glioma-associated protein SETA interacts with AIP1/Alix and ALG-2 and modulates apoptosis in astrocytes. *J. Biol. Chem.* 275:19275–19281.

Cheng, Z.J., R.D. Singh, D.K. Sharma, E.L. Holicky, K. Hanada, D.L. Marks, and R.E. Pagano. 2006. Distinct mechanisms of clathrin-independent endocytosis have unique sphingolipid requirements. *Mol. Biol. Cell.* 17:3197–3210.

Cormont, M., I. Meton, M. Mari, P. Monzo, F. Keslair, C. Gaskin, T.E. McGraw, and Y. Le Marchand-Brustel. 2003. CD2AP/CMS regulates endosome morphology and traffic to the degradative pathway through its interaction with Rab4 and c-Cbl. *Traffic.* 4:97–112.

Cover, T.L., and M.J. Blaser. 1992. Purification and characterization of the vacuolating toxin from *Helicobacter pylori. J. Biol. Chem.* 267:10570–10575.

de Bernard, M., E. Papini, V. de Filippis, E. Gottardi, J. Telford, R. Manetti, A. Fontana, R. Rappuoli, and C. Montecucco. 1995. Low pH activates the vacuolating toxin of *Helicobacter pylori*, which becomes acid and pepsin resistant. *J. Biol. Chem.* 270:23937–23940.

Dikic, I. 2002. CIN85/CMS family of adaptor molecules. *FEBS Lett.* 529:110–115.

Dustin, M.L., M.W. Olszowy, A.D. Holdorf, J. Li, S. Bromley, N. Desai, P. Widder, F. Rosenberger, P.A. van der Merwe, P.M. Allen, and A.S. Shaw. 1998. A novel adaptor protein orchestrates receptor patterning and cytoskeletal polarity in T-cell contacts. *Cell.* 94:667–677.

Engqvist-Goldstein, A.E., and D.G. Drubin. 2003. Actin assembly and endocytosis: from yeast to mammals. *Annu. Rev. Cell Dev. Biol.* 19:287–332.

Falnes, P.O., and K. Sandvig. 2000. Penetration of protein toxins into cells. *Curr. Opin. Cell Biol.* 12:407–413.

Galmiche, A., J. Rassow, A. Doye, S. Cagnol, J.C. Chambard, S. Contamin, V. de Thillot, I. Just, V. Ricci, E. Solcia, et al. 2000. The N-terminal 34 kDa fragment of *Helicobacter pylori* vacuolating cytotoxin targets mitochondria and induces cytochrome c release. *EMBO J.* 19:6361–6370.

Garner, J.A., and T.L. Cover. 1996. Binding and internalization of the *Helicobacter pylori* vacuolating cytotoxin by epithelial cells. *Infect. Immun.* 64:4197–4203.

Gauthier, N.C., V. Ricci, P. Gounon, A. Doye, M. Tauc, P. Poujeol, and P. Boquet. 2004. Glycosylphosphatidylinositol-anchored proteins and actin cytoskeleton modulate chloride transport by channels formed by the *Helicobacter pylori* vacuolating cytotoxin VacA in HeLa cells. *J. Biol. Chem.* 279:9481–9489.

Gauthier, N.C., P. Monzo, V. Kaddai, A. Doye, V. Ricci, and P. Boquet. 2005. *Helicobacter pylori* VacA cytotoxin: a probe for a clathrin-independent and Cdc42-dependent pinocytic pathway routed to late endosomes. *Mol. Biol. Cell.* 16:4852–4866.

Gruenberg, J., and H. Stenmark. 2004. The biogenesis of multivesicular endosomes. *Nat. Rev. Mol. Cell Biol.* 5:317–323.

Guerriero, C.J., K.M. Weixel, J.R. Bruns, and O.A. Weisz. 2006. Phosphatidylinositol 5-kinase stimulates apical biosynthetic delivery via an Arp2/3-dependent mechanism. *J. Biol. Chem.* 281:15376–15384.

Hutchings, N.J., N. Clarkson, R. Chalkley, A.N. Barclay, and M.H. Brown. 2003. Linking the T cell surface protein CD2 to the actin-capping protein CAPZ via CMS and CIN85. *J. Biol. Chem.* 278:22396–22403.

Kaksonen, M., C.P. Toret, and D.G. Drubin. 2005. A modular design for the clathrin- and actin-mediated endocytosis machinery. *Cell.* 123:305–320.

Kalia, M., S. Kumari, R. Chadda, M.M. Hill, R.G. Parton, and S. Mayor. 2006. Arf6-independent GPI-anchored protein-enriched early endosomal compartments fuse with sorting endosomes via a Rab5/phosphatidylinositol-3′-kinase-dependent machinery. *Mol. Biol. Cell.* 17:3689–3704.

Kim, J.M., H. Wu, G. Green, C.A. Winkler, J.B. Kopp, J.H. Miner, E.R. Unanue, and A.S. Shaw. 2003. CD2-associated protein haploinsufficiency is linked to glomerular disease susceptibility. *Science.* 300:1298–1300.

Kirsch, K.H., M.M. Georgescu, S. Ishimaru, and H. Hanafusa. 1999. CMS: an adapter molecule involved in cytoskeletal rearrangements. *Proc. Natl. Acad. Sci. USA.* 96:6211–6216.

Kobayashi, S., A. Sawano, Y. Nojima, M. Shibuya, and Y. Maru. 2004. The c-Cbl/CD2AP complex regulates VEGF-induced endocytosis and degradation of Flt-1 (VEGFR-1). *FASEB J.* 18:929–931.

Kurakin, A.V., S. Wu, and D.E. Bredesen. 2003. Atypical recognition consensus of CIN85/SETA/Ruk SH3 domains revealed by target-assisted iterative screening. *J. Biol. Chem.* 278:34102–34109.

Lacayo, C.I., and J.A. Theriot. 2004. *Listeria monocytogenes* actin-based motility varies depending on subcellular location: a kinematic probe for cytoarchitecture. *Mol. Biol. Cell.* 15:2164–2175.

Lee, K.H., A.R. Dinner, C. Tu, G. Campi, S. Raychaudhuri, R. Varma, T.N. Sims, W.R. Burack, H. Wu, J. Wang, et al. 2003. The immunological synapse balances T cell receptor signaling and degradation. *Science.* 302:1218–1222.

Lehtonen, S., F. Zhao, and E. Lehtonen. 2002. CD2-associated protein directly interacts with the actin cytoskeleton. *Am. J. Physiol. Renal Physiol.* 283: F734–F743.

Li, Y., A. Wandinger-Ness, J.R. Goldenring, and T.L. Cover. 2004. Clustering and redistribution of late endocytic compartments in response to *Helicobacter pylori* vacuolating toxin. *Mol. Biol. Cell.* 15:1946–1959.

Lord, J.M., and L.M. Roberts. 1998. Toxin entry: retrograde transport through the secretory pathway. *J. Cell Biol.* 140:733–736.

Lynch, D.K., S.C. Winata, R.J. Lyons, W.E. Hughes, G.M. Lehrbach, V. Wasinger, G. Corthals, S. Cordwell, and R.J. Daly. 2003. A Cortactin-CD2-associated protein (CD2AP) complex provides a novel link between epidermal growth factor receptor endocytosis and the actin cytoskeleton. *J. Biol. Chem.* 278:21805–21813.

Mayor, S., and H. Riezman. 2004. Sorting GPI-anchored proteins. *Nat. Rev. Mol. Cell Biol.* 5:110–120.

Merrifield, C.J., S.E. Moss, C. Ballestrem, B.A. Imhof, G. Giese, I. Wunderlich, and W. Almers. 1999. Endocytic vesicles move at the tips of actin tails in cultured mast cells. *Nat. Cell Biol.* 1:72–74.

Miceli, M.C., M. Moran, C.D. Chung, V.P. Patel, T. Low, and W. Zinnanti. 2001. Co-stimulation and counter-stimulation: lipid raft clustering controls TCR signaling and functional outcomes. *Semin. Immunol.* 13:115–128.

Monzo, P., N.C. Gauthier, F. Keslair, A. Loubat, C.M. Field, Y. Le Marchand-Brustel, and M. Cormont. 2005. Clues to CD2-associated protein involvement in cytokinesis. *Mol. Biol. Cell.* 16:2891–2902.

Moya, M., A. Dautry-Varsat, B. Goud, D. Louvard, and P. Boquet. 1985. Inhibition of coated pit formation in Hep2 cells blocks the cytotoxicity of diphtheria toxin but not that of ricin toxin. *J. Cell Biol.* 101:548–559.

Ng, M.M., F. Chang, and D.R. Burgess. 2005. Movement of membrane domains and requirement of membrane signaling molecules for cytokinesis. *Dev. Cell.* 9:781–790.

Papini, E., M. de Bernard, E. Milia, M. Bugnoli, M. Zerial, R. Rappuoli, and C. Montecucco. 1994. Cellular vacuoles induced by *Helicobacter pylori* originate from late endosomal compartments. *Proc. Natl. Acad. Sci. USA.* 91:9720–9724.

Patel, H.K., D.C. Willhite, R.M. Patel, D. Ye, C.L. Williams, E.M. Torres, K.B. Marty, R.A. MacDonald, and S.R. Blanke. 2002. Plasma membrane cholesterol modulates cellular vacuolation induced by the *Helicobacter pylori* vacuolating cytotoxin. *Infect. Immun.* 70:4112–4123.

Petrelli, A., G.F. Gilestro, S. Lanzardo, P.M. Comoglio, N. Migone, and S. Giordano. 2002. The endophilin-CIN85-Cbl complex mediates ligand-dependent downregulation of c-Met. *Nature.* 416:187–190.

Ricci, V., A. Galmiche, A. Doye, V. Necchi, E. Solcia, and P. Boquet. 2000. High cell sensitivity to *Helicobacter pylori* VacA toxin depends on a GPI-anchored protein and is not blocked by inhibition of the clathrin-mediated pathway of endocytosis. *Mol. Biol. Cell.* 11:3897–3909.

Rink, J., E. Ghigo, Y. Kalaidzidis, and M. Zerial. 2005. Rab conversion as a mechanism of progression from early to late endosomes. *Cell.* 122:735–749.

Sabharanjak, S., P. Sharma, R.G. Parton, and S. Mayor. 2002. GPI-anchored proteins are delivered to recycling endosomes via a cdc42-regulated, clathrin-independent pinocytic pathway. *Dev. Cell.* 2:411–423.

Schafer, D.A., C. D'Souza-Schorey, and J.A. Cooper. 2000. Actin assembly at membranes controlled by ARF6. *Traffic.* 1:892–903.

Schraw, W., Y. Li, M.S. McClain, F.G. van der Goot, and T.L. Cover. 2002. Association of *Helicobacter pylori* vacuolating toxin (VacA) with lipid rafts. *J. Biol. Chem.* 277:34642–34650.

Sharma, P., R. Varma, R.C. Sarasij, Ira, K. Gousset, G. Krishnamoorthy, M. Rao, and S. Mayor. 2004. Nanoscale organization of multiple GPI-anchored proteins in living cell membranes. *Cell.* 116:577–589.

Simpson, F., N.K. Hussain, B. Qualmann, R.B. Kelly, B.K. Kay, P.S. McPherson, and S.L. Schmid. 1999. SH3-domain-containing proteins function at distinct steps in clathrin-coated vesicle formation. *Nat. Cell Biol.* 1:119–124.

Soubeyran, P., K. Kowanetz, I. Szymkiewicz, W.Y. Langdon, and I. Dikic. 2002. Cbl-CIN85-endophilin complex mediates ligand-induced downregulation of EGF receptors. *Nature.* 416:183–187.

Taunton, J., B.A. Rowing, M.L. Coughlin, M. Wu, R.T. Moon, T.J. Mitchison, and C.A. Larabell. 2000. Actin-dependant propulsion of endosomes and lysosomes by recruitment of N-WASP. *J. Cell Biol.* 148:519–530.

Welch, M.D., and R.D. Mullins. 2002. Cellular control of actin nucleation. *Annu. Rev. Cell Dev. Biol.* 18:247–288.

Welsch, T., N. Endlich, W. Kriz, and K. Endlich. 2001. CD2AP and p130Cas localize to different F-actin structures in podocytes. *Am. J. Physiol. Renal Physiol.* 281:F769–F777.

Welsch, T., N. Endlich, G. Gokce, E. Doroshenko, J.C. Simpson, W. Kriz, A.S. Shaw, and K. Endlich. 2005. Association of CD2AP with dynamic actin on vesicles in podocytes. *Am. J. Physiol. Renal Physiol.* 289:F1134–F1143.

Yahiro, K., T. Niidome, M. Kimura, T. Hatakeyama, H. Aoyagi, H. Kurazono, K. Imagawa, A. Wada, J. Moss, and T. Hirayama. 1999. Activation of *Helicobacter pylori* VacA toxin by alkaline or acid conditions increases its binding to a 250-kDa receptor protein-tyrosine phosphatase beta. *J. Biol. Chem.* 274:36693–36699.

Zhang, A.S., A.D. Sheftel, and P. Ponka. 2005. Intracellular kinetics of iron in reticulocytes: evidence for endosome involvement in iron targeting to mitochondria. *Blood.* 105:368–375.